Stem Cell Research 56 (2021) 102513

Contents lists available at ScienceDirect

Stem Cell Research

journal homepage: www.elsevier.com/locate/scr

Cdkn1a deletion or suppression by cyclic stretch enhance the osteogenic potential of bone marrow mesenchymal stem cell-derived cultures

Cassandra M. Juran [a], Justina Zvirblyte [a,b], Margareth Cheng-Campbell [a,c], Elizabeth A. Blaber [a,c], Eduardo A.C. Almeida [d,*]

[a] Blue Marble Space Institute of Science at NASA Ames Research Center, Mountain View, CA 94043, USA
[b] Sector of Microtechnologies, Institute of Biotechnology, Life Sciences Center, Vilnius University, Sauletekio av. 7, LT-10257 Vilnius, Lithuania
[c] Center for Biotechnology and Interdisciplinary Studies, Department of Biomedical Engineering, Rensselaer Polytechnic Institute, Troy, NY 12180, USA
[d] NASA Ames Research Center, Moffett Field, CA 94035, USA

ARTICLE INFO

Keywords:
Mechanotransduction
Mesenchymal stem cells
Single cell transcriptomics
CDKN1A/P21
Cyclic stretch loading
Regeneration

ABSTRACT

CDKN1A/P21 is a potent inhibitor of cell cycle progression and its overexpression is thought to be associated with inhibition of normal bone regenerative osteogenesis during spaceflight. To test whether CDKN1A/P21 regulates osteogenesis in response to mechanical loading we studied cyclic stretch versus static culture of *Cdkn1a*$^{-/-}$ (null) or wildtype primary mouse bone marrow osteoprogenitors during 21-day *ex-vivo* mineralization assays. Cyclically stretched *Cdkn1a*$^{-/-}$ cells are 3.95-fold more proliferative than wildtype, while static *Cdkn1a*$^{-/-}$ cells show a 2.50-fold increase. Furthermore, stage-specific single cell RNAseq analyses show expression of *Cdkn1a* is strongly suppressed by cyclic stretch in early and late osteoblasts, and minimally in the progenitor population. Lastly, both stretch and/or *Cdkn1a* deletion cause population shift from osteoprogenitors to osteoblasts, also indicating increased differentiation. Collectively, our results support the hypothesis that *Cdkn1a* constitutively plays a mechano-reversible anti-proliferative role during osteogenesis and suggests a new molecular target to counter regenerative deficits caused by disuse.

1. Introduction

Mechanical stimulation of tissues has long been understood to play a significant role in promoting regeneration and in regulating proliferation and differentiation of adult stem cells (D'Angelo et al., 2011; Vining and Mooney, 2017). Reduced tissue mechanical stimulation, due to disuse on Earth or in microgravity, can disrupt homeostatic regenerative processes in multiple systems. The current understanding of tissue level stem cell regenerative processes has led investigators to focus on how mechanical stimulation elicits mechanotransduction pathways and alters the course of cell cycle progression in self-renewal or activation of proliferation and differentiation programs (Swift et al., 2013). *In-vivo,* stem cells exist within tightly regulated localized niche environments, which support stem cell multipotency (Wagers, 2012) and biophysical stresses can disrupt or maintain those niche environments by eliciting signaling that promotes transition from quiescence to active stem cell self-renewal, proliferation or differentiation (Stavenschi et al., 2018).

For our studies we focused on the bone marrow compartment because of its role in regenerative health and its experiencing frequent ambulation-related cyclical loading (Thomas and El Haj, 1996; Titushkin and Cho, 2007). *In-vivo* exercise physiology studies have established that bone fracture healing is dependent on mechanical conditions (Lanyon et al., 1982; Wallace et al., 2015) with ambulatory loading increasing regenerate bone volume and improving mechanical properties of the repaired bone (Boerckel et al., 2012). Conversely, studies of unloading disuse from a variety of post-operative recovery, bed rest, aging and spaceflight studies provide evidence that unloading results in catabolic imbalance of stem cell-based regenerative homeostasis (Akima et al., 2007; Berg et al., 2007; Riley et al., 2000). This imbalance can result in musculoskeletal wasting, reduction of bone mass, immune suppression, and the development of anemia (Perhonen et al., 2001; Takata et al., 1993).

Spaceflight specifically offers a uniquely sensitive experimental platform for studying the biological effects of mechanical unloading in bone, including our laboratory's early work which demonstrated the inhibition of osteogenesis and bone formation in space using the growing rat model (Morey and Baylink, 1978). Furthermore, microgravity's effect on the regenerative mechanisms of somatic and adult

* Corresponding author.
E-mail address: e.almeida@nasa.gov (E.A.C. Almeida).

https://doi.org/10.1016/j.scr.2021.102513
Received 18 February 2021; Received in revised form 8 August 2021; Accepted 19 August 2021
Available online 26 August 2021

progenitor stem cells, as well as its regulation of differentiation-related genes, have also been studied by our laboratory in cells isolated from the pelvic ilia bone marrow of 15-day space-flown mice (Blaber et al., 2014; Blaber et al., 2013). Those studies show that spaceflight suppressed pro-osteogenic growth and proliferation genes and identified a cell cycle inhibitor gene, *Cdkn1a*, as significantly upregulated in a whole bone heterogeneous cell population. In addition, increased CDKN1A/P21 protein was also immuno-detected along the periosteal surface niche of the proximal femur in space-flown mice. The cells of this niche can serve as a quiescent osteoblastic progenitor reservoir for load-induced osteogenic development (Bellosta et al., 2003), suggesting a role for CDKN1A/P21 in regulating quiescence of a mechano-activatable proliferative cell pool.

CDKN1A/P21 is a potent cyclin-dependent kinase inhibitor protein encoded by the *Cdkn1a* gene that promotes cell cycle arrest, by binding to, and inhibiting the activity of cyclin-CDK2, -CDK1, and -CDK4/6 complexes, thus promoting exit from the cell cycle for differentiation, proliferative arrest, or apoptosis (Cazzalini et al., 2010; Karimian et al., 2016). Although many studies focus on DNA damage or reactive oxygen species (ROS)-inducible *Cdkn1a* expression, persistent elevated levels of CDKN1A/P21 are often also observed in differentiated cells of various tissues, reflecting an additional role of CDKN1A/P21 in mediating cell cycle arrest in terminal differentiation (Gartel et al., 1996; Parker et al., 1995). Remarkably, mice that have a *Cdkn1a* homozygous deletion ($Cdkn1a^{-/-}$) show increased regenerative capacity, with the ability to re-pattern severed digits and close ear-hole punches without scaring (Bedelbaeva et al., 2010). Deletion of *Cdkn1a* also significantly decreases proliferative arrest susceptibility in response to DNA damage or replicative stresses, allowing for proliferation to proceed even when DNA damage may be present in the G1 phase of the cell cycle (Choudhury et al., 2007; Deng et al., 1995; Yosef et al., 2017).

Overall, these studies demonstrate the importance of CDKN1A/P21 as a regulator of cell cycle progression in adult stem cells during tissue regeneration, and suggest that *Cdkn1a* expression might be regulated by alterations in mechanical loading, particularly in mesenchymal stem cell-derived osteogenic progenitor and osteoblast pools of the bone marrow. Thus, we hypothesize that CDKN1A/P21 may be part of a molecular mechanism regulating bone regenerative osteogenesis in response to physiologic mechanical loading or unloading. To address this hypothesis, we investigated how the deletion of *Cdkn1a* changes the *ex-vivo* regenerative responses of bone marrow stem cell-derived osteoprogenitors to physiologically relevant mechanical stimulation with 21-days of cyclic stretch in osteogenic cultures. Stretch is a suitable model for our studies because it promotes osteoprogenitor growth and differentiation independently of soluble growth factors and is representative of compressive and bending cyclic loading incurred on the periosteal and endosteal surfaces occupied by these cells during gravity loading activity including weight bearing and ambulation (Haasper et al., 2008; Stavenschi et al., 2018; Titushkin and Cho, 2007). This study also assesses, at the single cell level, how mechanical loading alters gene expression of *Cdkn1a* throughout the different stages of osteogenic differentiation.

2. Materials and Methods

2.1. Cyclic Stretch Culture Chamber Assembly

Our study utilized a custom-built uniaxial cyclic stretch cell culture chamber, consisting of a loading frame, culture chambers, and a computer controlled 350 mA linear step motors with rubber insulation to inhibit heat transfer to the culture area (Searby, 2002). We clamped a 50 x 100 mm 0.25 mm thick platinum cured silicone thin film (The Rubber Company, Hampshire UK) and pre-strained it to 5 mm tensile deformation defined as the zero-position. Nunc 4-well chamber slides (Thermo Scientific Nunc Chamber Slides, 1.8 cm^2/well) were detached from their imaging slide and the culture well chamber was mounted to the pre-strained silicone thin film. Cyclic linear uniaxial loading was applied by step motors using an Arduino Uno microcontroller as described in Figure S1(A-C).

2.2. Ethics Statement

All animal work was approved by the Institutional Animal Care and Use Committee at National Aeronautics and Space Administration (NASA) Ames Research Center, and conformed to the US National Institutes of Health Guide for the Care and Use of Laboratory Animals.

2.3. Bone Marrow Stem Cell Isolation

Bone marrow osteoprogenitor cells were isolated from the femur and tibia of 16 to 18 week-old $Cdkn1a^{-/-}$ and wildtype (B6129SF2J) male mice (The Jackson Laboratory, Maine). Within 5 minutes of dissection, tibias and femurs were cut open and flushed with 3 ml of osteogenic medium (Minimum Essential Medium (MEM) Alpha Medium (Gibco) with 15% fetal bovine serum and 1% Antibiotic-Antimycotic solution (Gibco)) per bone. Cells were assessed for viability using trypan blue, and red blood cells lysed with RBC lysis buffer (Invitrogen) for 10 minutes at room temperature, followed by centrifugation and re-suspension in 4 ml osteoblastic (OB) medium (osteogenic medium with 1% 1M beta glycerophosphate and 1% 5 mM ascorbic acid) and counted using a Bio-Rad TC20 cell counter. Cells were plated at 500,000 cells per well in 1.25 ml of OB medium (approximately 320,000 cells/cm^2) and maintained at 37℃ with 5% CO_2 with medium changes every 3 days.

2.4. Osteoblastogenesis and Cyclic Stretch Loading Culture

Cells were allowed to grow on the silicone substrate for 10 days of static growth before loading. Starting on day 11, the cultures underwent continuous cyclic uniaxial stretch at 0.1% maximum tensile strain (or 0.1 mm of deformation) at a frequency of 0.1 Hz (6 cycles/min or 5-sec stretch/5-sec relaxation)(Guyot et al., 2016). This loading regime was chosen to model a continuous dynamic weight bearing loading paradigm to test the hypothesis that cyclic loading suppresses constitutive *Cdkn1a* expression inhibiting proliferation during osteogenesis. Control cultures were held at the zero-position tension for the duration of the experiment. Our experimental design evaluates the various stages of osteoblast differentiation (progenitor proliferation, early osteoblast-mediated extracellular matrix deposition, and osteoblast-mediated hydroxyapatite deposition mineralization)(Fakhry et al., 2013) and correlates critical transitions with assessments at 7, 14 and 21-day culture time points (D7, D14, D21), (Figure S1(D)).

2.5. Cell Growth Analysis

Upon relevant culture conclusion, cell cultures were enzymatically dissociated with trypsin EDTA (Ethylenediaminetetraacetic acid) and assessed for viability using Trypan Blue exclusion. Dissociated cells were also fixed with RNALater (Thermo Fisher Scientific) and stored at -80℃ until analysis by qRT-PCR (see Supplementary Material Experimental Procedures). A subset of cultures was fixed for visualization with 2% glutaraldehyde for 60 seconds before three sequential PBS rinses for 5 minutes each. Samples were then processed for cell cycle profile staging with DAPI (ThermoFisher Scientific) staining for 2 minutes at 37℃, and images captured on an Olympus BX51 at two intensities and evaluated using CellProfiler (Broad Institute) following the protocol of (Roukos et al., 2015).

Bromodeoxyuridine/5-bromo-2'-deoxyuridine (BrdU) proliferation marker staining of D9 samples was conducted with an 18 hours antibody incubation and Horseradish peroxidase (HRP)/DAB streptavidin-biotin detection. The QuPath (Broad Institute) application's positive cell identification toolkit was used to quantify the percent positive cells.

2.6. Assessment of differentiation by mineralization imaging

Cultures were fixed with 100% ethanol for 5 minutes and left to dry overnight. The cultures were rehydrated in PBS for 5 minutes repeated 3 times before von Kossa mineralization assay assessment (see Supplementary Material Experimental Procedures). The Von Kossa samples were analyzed for mineralized area using the ImageJ particle analyzer for nodule % Area. Von Kossa stained mineralized images were also assessed for three-dimensionality by quantifying optical density (I/I_0). For further details see Supplementary Material Experimental Procedures. A subset of Von Kossa stained wells were counterstained with Toluidine Blue to identify nuclei. Histologic bright field images were captured on a Zeiss AxioSkop 2 Plus, and evaluated for mineralized matrix morphology.

2.7. Proliferative Capacity of late mineralizing osteoblasts re-plating assessment

After a 21-day static osteogenic culture, wildtype and *Cdkn1a*$^{-/-}$ cells in 12-well culture plates were dissociated from mineralized nodules by trypsin EDTA, counted and re-plated into collagen wells. After 3 hours, adhesion of dissociated cells was imaged. After an additional 45 hours of culture (48 hours post-replating) cultures were again imaged and then dissociated using trypsin EDTA and counted to assess proliferation.

2.8. Single cell RNA-Sequencing (scRNA-seq) and subsequent 10X Genomics CellRanger analysis

For single cell analyses bone marrow osteoprogenitors from four *Cdkn1a*$^{-/-}$ and wildtype animals were isolated, as described above, and cultured unstimulated for 7 days and then cyclically stretched at 0.1% strain and 0.1 Hz continuously for 48 hours (cells from n = 4 mice per genotype and sourced cells were cultured for both static control and cyclic stretch). After 48 hours of stimulation the cells were dissociated with trypsin and EDTA (Gibco) and washed with 0.04% bovine serum albumin (BSA) (Thermo Fisher Scientific) in PBS. Cell suspension were passed through Flow-mi cell strainer (Bel-Art), to achieve single cell suspensions. scRNA-seq libraries were prepared according to the 10X Genomics single cell Gene Expression Profiling v3 chemistry protocol (10X Genomics). Libraries were sequenced by the NASA GeneLab Sequencing Group at NASA Ames Research Center (Moffett Field, CA) on a NovaSeq 6000 using an S2 Xp 2-lane kit paired end 100 (PE 100) configuration. Final read summary metrics indicated 25,890 total cells were identified in the four libraries: Wildtype static control, Wildtype cyclic stretch, *Cdkn1a*$^{-/-}$ static control and *Cdkn1a*$^{-/-}$ cyclic stretch with a median of 2,097 genes identified per cell. Quality assessment, log-2-fold change differential expression and statistical analysis (normalization, dimensionality reduction, clustering and differential expression) of the scRNA-seq results were done utilizing the 10X Genomics CellRanger v3.1.0 toolkit and several R analyses packages (manipulation of the matrix raw data was conducted utilizing Seurat, gdata, and Bioconductor packages) and visualization with the Loupe cell browser v4.0.0 (10X Genomics). To study osteogenesis heterogeneity in the single cell libraries, we utilized a biomarker guided clustering paradigm to segregate cells belonging to progenitor, early proliferative and late mineralizing osteoblast cell populations. For further description of Biomarker panel see Supplementary Material Experimental Procedures.

2.9. Statistics

Each experiment was replicated on at least nine separate occasions. Cell count, doubling time, and trypan blue % live data was collected from aliquots of two wells from 4 of the 9 replications of the experiment (n=8). The same samples were then suspended in RNALater and used for RT-PCR analysis. Individual gene expression was analyzed in triplicate from a minimum of 3 sample suspensions (n`=6 assessed in triplicate). For all imaging analysis, each staining was performed on 2 wells from 3 of the 9 replications and 3 images collected per sample were averaged (n=6 assessed in triplicate). Statistical significance was assigned using paired t-test to detect differences between the genotypes at a single time point. Then the differences between cyclic stretch and static control conditions within the genotype were detected using a one-way repeated measures analysis of variance (ANOVA) followed by a multiple-comparisons test with a Sidak's adjustment post hoc, establishing significance with p value 0.05 or less and, 2-way analysis of variance (ANOVA) followed for multiple-comparison tests with Tukey Kramer (Tukey HSD) adjustments post hoc establishing significance with p value 0.05 or less.

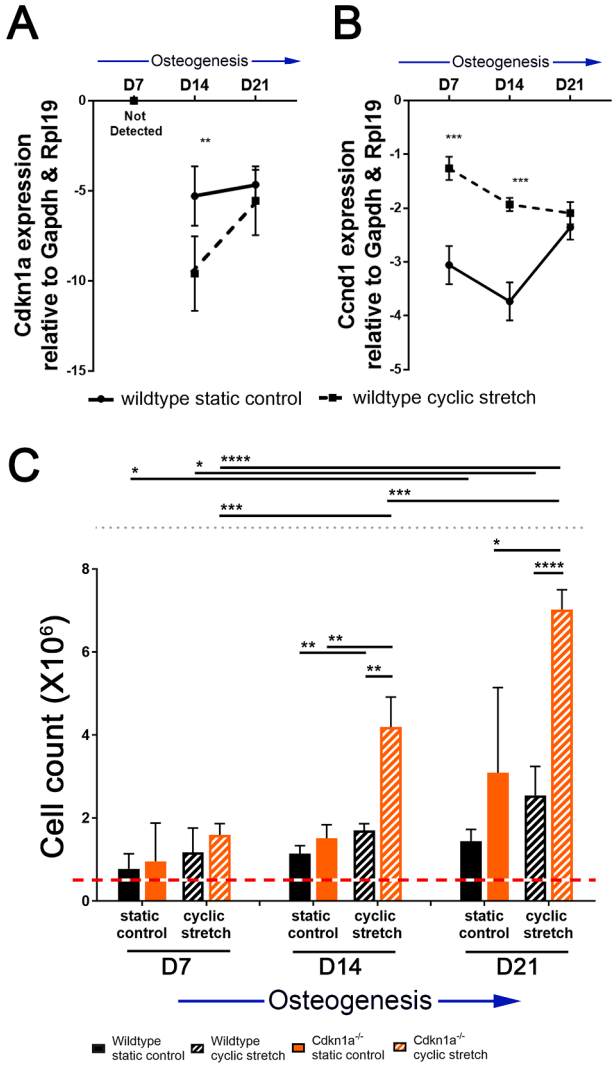

Figure 1. Cyclic stretch suppresses *Cdkn1a* expression in wildtype osteogenic cultures and promotes a hyper-proliferative response in *Cdkn1a*$^{-/-}$ cultures. Cyclic stretch leads to decreases in *Cdkn1a* expression at D14 of osteogenesis (A) while *Ccnd1* expression is increased at D7 and D14 (B) in the wildtype osteogenesis culture (ΔCt gene of interest compared to the average of *Rpl19* and *Gapdh* housekeeping genes). C) Quantification of cell count data during the osteogenesis culture shows that cyclic stretch increases cell count in wildtype cells and that the deletion of *Cdkn1a* greatly increases the magnitude of the proliferative response to stretch. (n=8, *p<0.1, **p<0.05, ***p<0.01, ****p<0.001, dashed line indicates initial seeding density, 500,000 cells)

3. Results

3.1. Coupled Cdkn1a suppression and Ccnd1/Cyclin D stimulation of gene expression induced by mechanical loading result in elevated cell proliferation during osteogenesis.

To assess the role of mechanical stimulation in regulating cell cycle progression during osteogenesis, we evaluated expression of the *Cdkn1a* and *Ccnd1* genes by qRT-PCR with and without stretch throughout 21-days of osteogenic culture undergoing *in-vitro* mineralization (Figure 1A). *Cdkn1a* mRNA in whole cultures becomes readily detectable at D14 with cyclic stretch suppressing levels of expression 1.81-fold from static control. By day 21 (D21) *Cdkn1a* expression is independent of mechanical loading. Figure 1B shows *Ccnd1* expression is elevated with cyclic stretch at D7 and D14 (2.42-fold and 1.93-fold respectively). At D21, proliferative increases associated with cyclic stretch are reduced, with the onset of osteoblast maturation, and no difference in *Ccnd1* expression is observed relative to static controls. Together, the expression patterns of *Cdkn1a* and *Ccnd1* are consistent with elevated cell count data in the wildtype cyclic stretch cultures (Figure 1C). Specifically, at D7 wildtype cells appear predominantly proliferative and no statistical difference is observed in cell count between static control and cyclic stretch cultures. At D14 however the cyclic stretch cell count is 1.5X higher than the static control and at D21, cyclic stretch results in cell counts elevated 1.76X.

3.2. Deletion of Cdkn1a magnifies mechanical load-induced increases in osteoprogenitor proliferation during osteogenesis

The deletion of *Cdkn1a* increases the proliferative rate (linear regression slope ratio) of osteoprogenitors by 2.60X relative to wildtype in static control cultures. Between D7 and D21 *Cdkn1a*$^{-/-}$ cells respond to cyclic stretch with increased proliferation (1.67X, 2.78X and 2.27X respectively). Comparison of the D21 cell count growth rate of cyclically stretched *Cdkn1a*$^{-/-}$ cells relative to cyclically stretched wildtype cells results in a 3.95X increase, and a striking 8.5X increased growth rate of the *Cdkn1a*$^{-/-}$ cyclic stretch cultures compared to wildtype static controls.

To further elucidate the proliferative features of *Cdkn1a*$^{-/-}$ cells, we investigated cell cycle progression using DAPI (4′,6-diamidino-2-phenylindole) nuclear staining intensity, to determine DNA content per cell, then assigning the stage of cell cycle to each nucleus (Roukos et al., 2015). We used an imaging approach for cell cycle staging, rather than flow cytometry primarily to identify how cell cycle progression is related to localization in mineralizing nodules. In addition, we also used this method because dissociation of intact cells from mineralized nodules is difficult and can lead to cell disruption and bias in cell cycle staging of the culture.

Figure 2A shows representative D14 DAPI intensity micrographs used in profile analysis. Nuclear morphology of wildtype cells shows some flattened nuclei (indicative of non-proliferative spread cells) and many small condensed nuclei (characteristic of actively dividing rounded cells). The *Cdkn1a*$^{-/-}$ static control cells have more rounded nuclei than either of the wildtype conditions, but cyclic stretch induces almost exclusively rounded actively dividing cells. Corresponding D14 representative cell cycle profiles show the quantitative increase in nuclei identified as S-phase and G2/M phase in the *Cdkn1a*$^{-/-}$ genotype and especially in the cyclic stretch mechanical condition (Figure 2B-C). Figure 2D quantifies the percentage of cells in each stage of cell cycle throughout the 21-day osteogenesis protocol. Additional cell cycle profiles for D7 and D21 are included in Figure S2.

The progression of differentiation in wildtype static control cultures results in a gradual increase in the percentage of cells identified as G1, decreasing the percentage of cells in S and G2/M phase. Similarly, the *Cdkn1a*$^{-/-}$ static control cells show a shift of cells to G1; however, cyclic stretch in the *Cdkn1a*$^{-/-}$ culture results in a shift of cells identified as G1 and S to G2/M. The temporal elevation of *Cdkn1a*$^{-/-}$ cells in G2/M in response to cyclic stretch is significant between D7 and D21, with D21 having the highest percentage cells identified as G2/M phase, indicating active proliferation at late osteogenesis. Corresponding BrdU incorporation data for the three osteoblastogenesis time points is included in Figure S3 showing that the D21 *Cdkn1a*$^{-/-}$ cyclic stretch cells have approximately 30% BrdU positive cells in comparison to 15% for the *Cdkn1a*$^{-/-}$ static controls and below 7% BrdU positive cells for both wildtype conditions. In addition to cell cycle profile analysis and BrdU incorporation, we assessed percent live cells using the LIVE/DEAD cytotoxicity staining kit (Molecular Probes) and found no significant deviation in percent live cells between genotype in response to mechanical culture condition with the exception of D21 when *Cdkn1a*$^{-/-}$ cyclic stretch cultures had approximately 92% live cells compared to the cyclic stretch wildtype at approximately 62% (Figure S4). This is possibly due to higher proliferation in the null stretch condition.

3.3. Cdkn1a$^{-/-}$ cells show greater expression of osteogenic markers connexin 43 (Gja1), collagen type 1 (Col1a1) and Alkaline Phosphatase (Alpl)

To investigate the progression of osteoblastogenesis, we evaluated a panel of three key osteogenesis markers (Figure 3): *Gja1*, a marker of osteoblast intercellular networking crucial for bone development and remodeling; *Col1a1*, the major structural extracellular matrix protein of bone which has a peak expression during the transition of osteoprogenitors to early osteoblast commitment; and *Alpl*, a molecular marker of late-stage matrix maturation and mineralization by osteoblasts. qRT-PCR of the biomarker panel shows that cyclic stretch elevates *Gja1*, *Col1a1*, and *Alpl* expression in D21 wildtype maturing osteoblasts, indicating that stretch is a pro-osteogenic stimulant resulting in dense osteoblasts nodules being formed and maturing to mineralization. In *Cdkn1a*$^{-/-}$ cyclic stretch cultures, the expression patterns of the three marker molecules are increased compared to all other conditions, indicating that osteogenesis is highly inducible in response to cyclic stretch in the *Cdkn1a*$^{-/-}$ cells.

3.4. Mineralization is proportional to cell number but independent from Cdkn1a status

Von Kossa mineral staining area (percentage of total well area) is quantified in Figure 4A. Both genotypes mineralize matrix more readily when cyclic stretch is applied. At D7, cyclic stretch results in an increase of 6.05X and 1.81X mineralized area in the *Cdkn1a*$^{-/-}$ and wildtype cultures respectively. The wildtype cultures also have elevated mineralized area in response to cyclic stretch at D14 (2.46X), but at D21 the cyclic stretch culture has 0.88X the mineralized area of the static control, indicating the effects of cyclic stretch are prominent during the proliferative phase of the culture. In contrast, elevated measure of mineralized area in response to cyclic stretch remains in the *Cdkn1a*$^{-/-}$ cultures throughout osteogenesis due to the elevated mineralization in response to stretch and continued proliferative capacity of the null culture.

To address the three-dimensionality of osteogenic nodules we quantified light transmitted through the mineralized matrix (Figure 4B). Analysis shows that the *Cdkn1a*$^{-/-}$ cultures have denser nodules than wildtype and that both cultures have increased mineral density in response to cyclic stretch. However, when the mineral density of the cyclic stretch cultures was normalized against their respective static controls, genotype-related differential mineralization responses to stretch are eliminated. *Cdkn1a*$^{-/-}$ normalized mineralized densities are elevated by cyclic stretch 1.62X, 1.42X and 1.76X for D7, 14 and 21 respectively, comparable to wildtype normalized mineralized densities which are elevated 1.45X, 1.45X, and 1.72X (Figure S5). These data show that mineralization is independent of *Cdkn1a* status and suggests that the higher values of mineralized area and mineral density are due to

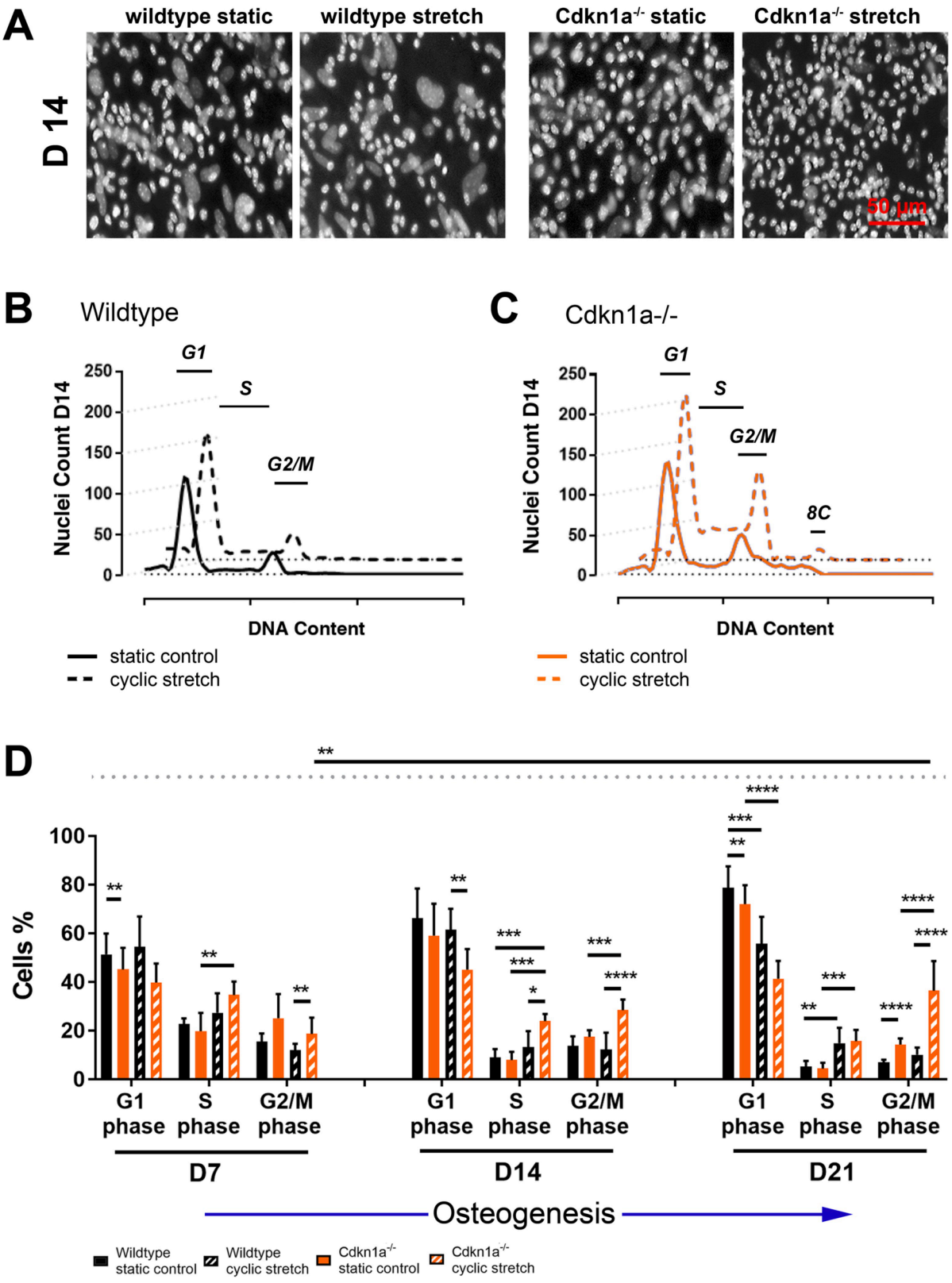

Figure 2. Cyclic Stretch promotes G1 to S phase transition and G2/M checkpoint accumulation in *Cdkn1a*$^{-/-}$ cells. A) D14 static and stretch nuclear morphology of wildtype and Cdkn1a$^{-/-}$ cells. Representative cell cycle profiles of the wildtype B) and *Cdkn1a*$^{-/-}$ C) cells at D14 in response to mechanical stimulation. D) Percentage of cells committed to each phase of cell cycle during osteogenesis showing cyclic stretch increases % cells in S-phase for both genotypes and that *Cdkn1a*$^{-/-}$ cells accumulate in G2/M phase. (n=8, *p<0.1, **p<0.05, ***p<0.01, ****p<0.001

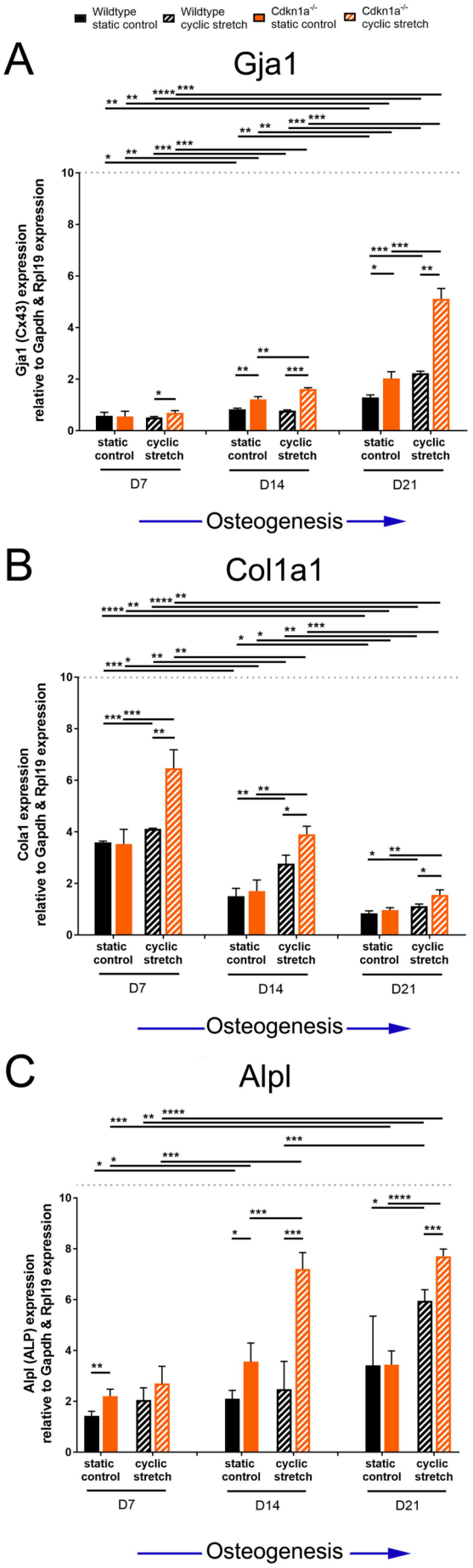

Figure 3. Expression of osteogenic development markers connexin 43 (*Gja1*), collagen type 1 (*Col1a1*) and alkaline phosphatase (*Alpl*). A) Quantification of *Gja1* shows increasing expression with progression of osteogenic culture in both *Cdkn1a*$^{-/-}$ and wildtype cells, with the *Cdkn1a*$^{-/-}$ cyclic stretch cells having a 5-fold increase. B) *Col1a1* expression is highest at D7 for both genotypes and mechanical conditions tested. Cyclic stretch induces retention of higher levels of *Col1a1* expression over time with the *Cdkn1a*$^{-/-}$ response to stretch retaining *Col1a1*'s highest expression levels. C) *Alpl* increases in expression with osteogenic culture. Cyclic stretch of *Cdkn1a*$^{-/-}$ cells accelerates elevated expression, such that at D14 the expression level is statistically indifferent to D21 values for both control and stretch cultures. (n=6, *p<0.1, **p<0.05, ***p<0.01, ****p<0.001)

mechanical stimulation and the increased cell numbers in the *Cdkn1a*$^{-/-}$ genotype. Histology of the mineral nodules, shown in Figure 4C-J, corroborates mineralized optical density data showing wildtype and *Cdkn1a*$^{-/-}$ cyclic stretch cells produce highly three-dimensional mineral by D21.

3.5. Cdkn1a$^{-/-}$*, but not wildtype, cells dissociated from mineralized 21-day osteogenic cultures show early proliferative capacity after re-plating*

At the end of the 21-day osteogenic culture, we sought to determine if late osteoblastic cells, enzymatically dissociated from mineralized nodules, retained progenitor-like proliferative capacity related to *Cdkn1a* status. To do this we dissociated D21 wildtype and *Cdkn1a*$^{-/-}$ static control cultures and re-plated the dissociated cells on collagen-coated dishes using osteogenic medium. Figure 5A shows that re-plated *Cdkn1a*$^{-/-}$ late-stage osteoblasts have a 5.22X increased cell count number after 48 hours of culture compared to wildtype. Images of cells recovered from mineralized nodules were comparable after 3 hours of initial adhesion for both the wildtype and *Cdkn1a*$^{-/-}$ cultures. However, after 48 hours, *Cdkn1a*$^{-/-}$ cells showed evident signs of proliferation and of nearing confluency, while wildtype cells remained at a density comparable to initial plating (Figure 5B). These results show that *Cdkn1a*$^{-/-}$ late mineralizing osteogenic cultures retain cells capable of active proliferation immediately after dissociation from mineralized nodules.

3.6. Single cell RNA sequencing (scRNA-seq) reveals Cdkn1a$^{-/-}$ *cells progress into late osteoblasts more efficiently than wildtype and that cyclic stretch shifts osteoprogenitors to early osteoblast commitment*

To further elucidate the role of CDKN1A/P21 in mechanoregulation of stem cell self-renewal, progenitor proliferation and osteogenic commitment to mineralizing phenotype, we used scRNA-seq at 9-days of osteogenesis commitment when wildtype static cell cultures contain about 2/3 progenitors and 1/3 already committed cells expressing various stages of osteoblast differentiation markers. To cluster single cells into osteogenic stages we characterized a panel of expressome biomarkers to assign populations of (osteo)progenitor cells (*Tnfrsf11a/Rank, Cd34*), early (proliferating) osteoblasts (*Bmp2, Runx2, Gja1, Col1a1, MMp13*), and late (mineralizing) osteoblasts (*Alpl, Bglap2, Bglap, Ibsp, Dmp1*) (Khayal et al., 2018). Using these staging biomarkers, we defined clusters of stage-specific single cells with highly related expressomes, visualized in Figure 6A.

The relative distribution of cell counts associated with each differentiation-stage cluster are quantified in Figure 6B. Staging shows that in the wildtype static control cultures, nearly 70% of cells are identified as osteoprogenitors, about 25% as early osteoblasts and about 5% as late osteoblasts. Cyclic stretch stimulation caused 27.0 ± 1.5% of wildtype progenitors to transition to the early osteoblast cluster, with no significant changes in the late osteoblast numbers. *Cdkn1a*$^{-/-}$ static cultures have fewer progenitors, more early osteoblasts and double the number of late osteoblasts. As with wildtype, stretch stimulation shifts

(caption on next column)

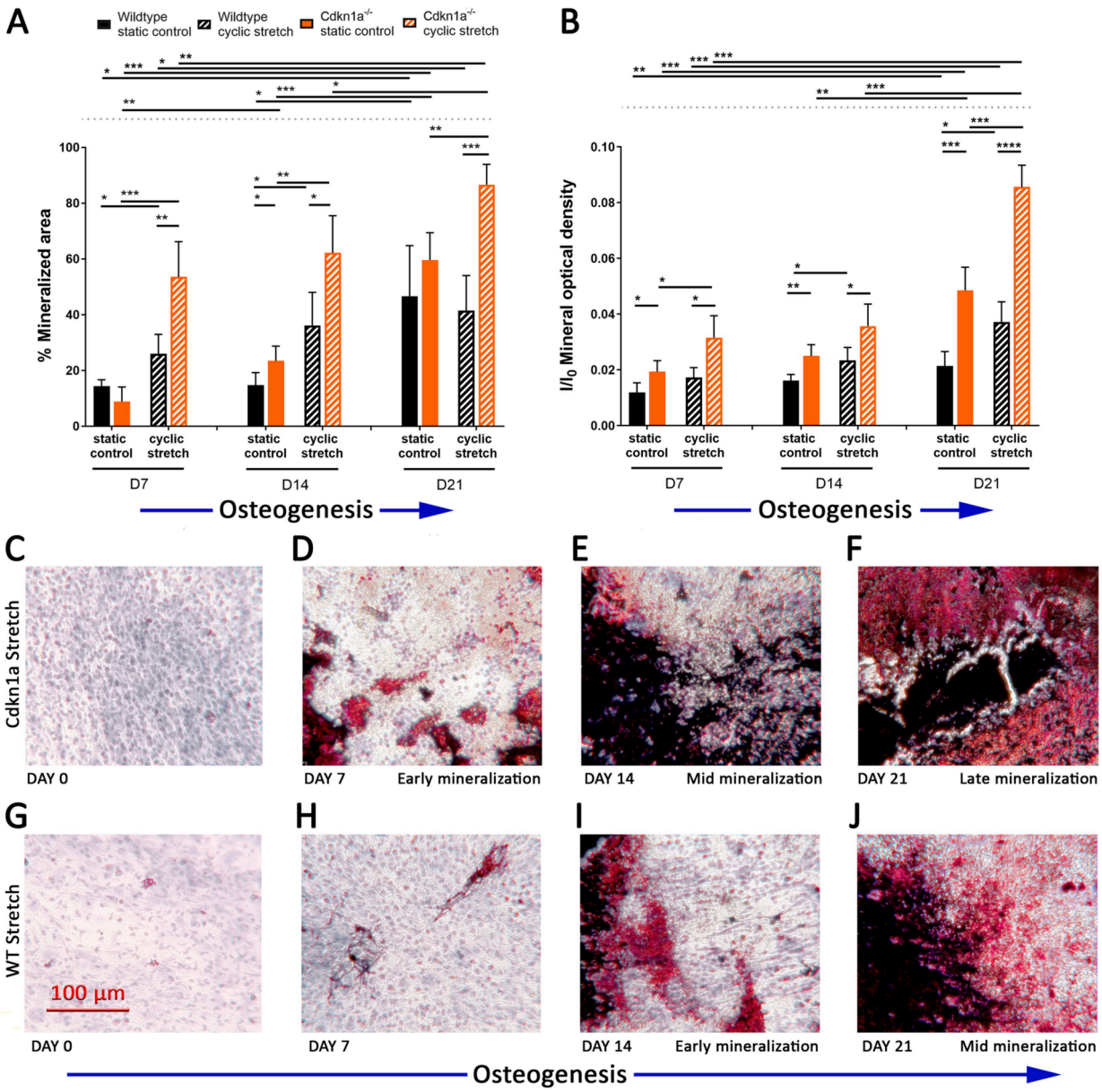

Figure 4. Mineralization is enhanced proportionally to cell number by cyclic stretch both in wildtype and *Cdkn1a*$^{-/-}$ cells. Functional assessment of mineral quality is presented in A) and B) and show cyclic stretch of *Cdkn1a*$^{-/-}$ cultures produces more mineral (area) and higher quality mineral (density) than the wildtype cells (n=6, *p<0.1, **p<0.05, ***p<0.01, ****p<0.001). C-J) Representative micrographs of mineral staining from the cyclic stretch cultures show the *Cdkn1a*$^{-/-}$ culture have greater cell density at D0 (from the same number of seeded cells), resulting in a "jumpstart" to mineralization by approximately 7 days (Early, Mid, and Late Mineralization labels).

Cdkn1a$^{-/-}$ cells from the progenitor cluster to the early osteoblast cluster with the late osteoblast cluster remaining unchanged. A visual depiction of the cluster expression patterns of three representative differentiation staging biomarkers (*Tnfrsf11a/Rank*, *Col1a1*, and *Ibsp*) for each genotype and loading condition are shown in Figure 6C with additional osteogenesis marker t-SNE plots used for cluster identification shown in Figure S6. Progenitor marker *Tnfrsf11a/Rank* shows consistent gene expression levels throughout the various conditions, suggesting that the features of this cluster do not change significantly with *Cdkn1a* deletion or load. In contrast, the early osteoblast cluster expression of *Col1a1* is highly dynamic showing a large decrease in expression with stretch in the wildtype but not *Cdkn1a*$^{-/-}$ cultures. At the D9 early osteogenesis timepoint, there is already a readily quantifiable population of late mineralizing osteoblasts (*Ibsp*+ cells) in both wildtype and *Cdkn1a*$^{-/-}$ cultures. In neither genotype is the percentage of *Ibsp*+ cells modulated by cyclic stretch, which is consistent with our mineralization assay results. However, *Cdkn1a*$^{-/-}$ late osteoblasts show elevated expression of *Ibsp* with mechanical stimulation, a feature not seen in the wildtype cells.

3.7. At the single cell level, cyclic stretch promotes proliferation in wildtype and Cdkn1a$^{-/-}$ *early osteoblasts but only Cdkn1a*$^{-/-}$ *cells show increased proliferation in the late osteoblast stage*

Single cell mapping of *Cdkn1a* expression in wildtype static control cells show early and late osteoblasts have elevated *Cdkn1a* associated with exit from cell cycle for commitment to osteoblast differentiation. Cyclic stretch mediated downregulation of *Cdkn1a* expression in the wildtype genotype at single cell resolution is shown in Figure 7A. Cyclic stretch reduces *Cdkn1a* expression in early and late osteoblast single cells to background levels. Further, wildtype cells that show suppression of *Cdkn1a* with stretch also show suppression of *Cirbp*, a p21 mRNA

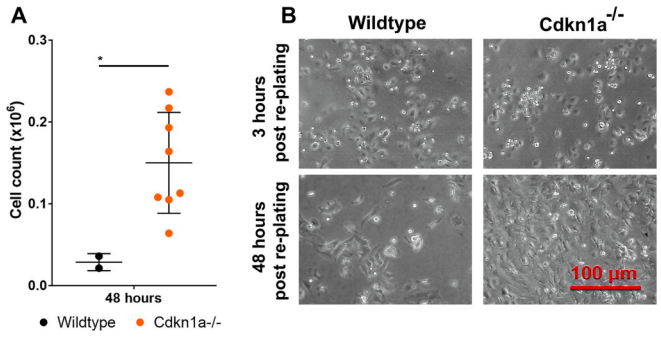

Figure 5. *Cdkn1a*$^{-/-}$ late mineralizing osteoblasts have elevated early proliferative capacity after dissociation and re-plating compared to Cdkn1a expressing wildtype. A) Cell count data after 48 hours of culture post re-plating, *Cdkn1a*$^{-/-}$ cells have 5.22X the cell count as wildtype controls. B) Visualization of the re-plated cultures show that three hours post-replating both wildtype and *Cdkn1a*$^{-/-}$ cultures have comparable appearance; However, at 48 hours post re-plating, only the *Cdkn1a*$^{-/-}$ cultures show increasing cellular density indicative of cell population expansion nearing confluency. In contrast, wildtype 48-hour re-plated cells have no indication of significant proliferative capacity, at the 48-hour early timepoint. (n=8, *p<0.1)

stability regulator (Figure 7C) plus elevated expression of *Ccnd1*/cyclin D (Figure 7D). Mechanical co-regulation of these genes is associated with increased proliferation mediated by cyclic stretch in the wildtype genotype.

Single cell mapping of static control *Cdkn1a*$^{-/-}$ cells show *Ccnd1*/cyclin D expression is elevated from the wildtype static control levels, especially in the late osteoblast cluster. Cyclic stretch of the *Cdkn1a*$^{-/-}$ cells results in elevated expression of *Ccnd1*/cyclin D in both the early and late osteoblast cell types, with the highest expression levels in a subpopulation of early osteoblasts. Representative Bromodeoxyuridine/5-bromo-2'-deoxyuridine (BrdU) staining of *Cdkn1a*$^{-/-}$ cultures show more BrdU-positive cells than seen in the wildtype as well as fewer large unstained nuclei indicative of proliferatively arrested cells. However, percent BrdU-positive quantitative data show BrdU incorporation is not changing with genotype or loading condition (Figure 7E). Detailed inspection of the cultures shows notable differences between the wildtype and *Cdkn1a*$^{-/-}$ cyclic stretch cells including BrdU incorporation in cells within the highly populated osteogenic nodules exclusively in the *Cdkn1a*$^{-/-}$ cultures. This finding confirms that *Cdkn1a*$^{-/-}$ cells in the mature mineralized nodule environment are still actively proliferating, a genotype dependent feature not evident in the wildtype static control or cyclic stretch cells.

4. Discussion

Although the broad concept that mechanical stimulation of tissues promotes stem cell-based tissue regenerative processes is generally accepted, a detailed mechanistic understanding of how this occurs is still lacking. A particularly important question is whether mechanical stimulation promotes stem cell derived osteoprogenitor proliferation, differentiation or both. Towards this goal, our study provides novel evidence that expression of the cell cycle regulator *Cdkn1a* limits both regenerative proliferation and differentiation in primary bone marrow osteogenic cultures and its expression is suppressed by mechanical stimulation, resulting in increased mineralized tissue formation. Additionally, this work establishes at the single cell level that mechanoregulation of *Cdkn1a* is not universal to all cell types in osteogenic cultures, but rather limited to those specialized beyond the progenitor state and committed to osteoblastic differentiation.

To examine the combined roles of mechanical stimulation and *Cdkn1a* status in osteogenesis, we used *Cdkn1a* null primary cells in a continuous cyclic stretch culture system, finding that its endogenous expression significantly blunts the proliferative and differentiation advantages of mechanical stimulation on osteogenic cultures. The proliferative capacity of the *Cdkn1a*$^{-/-}$ genotype in response to cyclic stretch eclipses the wildtype with 3.95X greater cell numbers than wildtype cyclic stretch and 8.5X increase versus wildtype static controls after an initial proliferative phase coincident to all osteogenic cultures. An assessment of mineralization shows that cyclic stretch increases the quantity and quality of mineralized matrix; however, the results were unable to resolve if *Cdkn1a* status directly impacts osteogenic differentiation, as the *Cdkn1a*$^{-/-}$ cyclic stretch culture accelerates nodule formation but also shows increased cell density, which may positively influence mineral production. To address this limitation, we conducted a single cell mRNAseq study at day 9 of osteogenic culture, when culture cell densities were similar for all studied conditions, thereby controlling for potential cell density effects on proliferation and differentiation and also presenting all relevant osteogenic cell stages. Single cell transcriptomics were able to resolve that cyclic stretch induces advancement of progenitor cells toward early and late osteoblast and that this transition is in concert with suppression of *Cdkn1a* in the wildtype committed osteoblasts. Further, *Cdkn1a* null status accelerates early to late osteoblast specialization, providing detailed evidence that *Cdkn1a* expression acts to limit both proliferative and differentiation mechanisms. These data, when paired with our previous findings that *Cdkn1a* expression in bone is upregulated as a result of spaceflight in microgravity, suggests a potential regulatory framework for how stem cell-based bone regenerative processes may be inhibited in space and in conditions of disuse on Earth.

Cell cycle profile analyses were also conducted to address how *Cdkn1a*$^{-/-}$ status affects osteogenesis, and they showed elevated S and G2/M identified cells, confirmed by increased BrdU incorporation, in the *Cdkn1a*$^{-/-}$ genotype and an earlier appearance of an 8C peak, indicative of endoreduplication (Dulić et al., 1998) (marker of disruption in DNA replication management). However, DNA damage in the absence of CDKN1A/P21 must be regulated by later cell cycle checkpoints, as loss of *Cdkn1a* alone does not significantly promote short-term increases in tumor formation or malignancy in mice compared to other tumor suppressor gene knockout models such as *Trp53* (Donehower et al., 1992; Martín-Caballero et al., 2001). The deletion of *Cdkn1a* does, however, increase the incidence of benign tumor formation, such as in skin papilloma (Jackson et al., 2002; Weinberg et al., 1999).

A shared molecular mechanism common to disuse in space and on Earth is the increased production of reactive oxygen species (ROS) and resulting oxidative stress. Elevated ROS presence in tissues exposed to spaceflight radiation and unloading stressors could trigger CDKN1A/P21-mediated cell cycle arrest during normal regenerative processes. Radiation exposure in spaceflight can further induce ROS formation in cells and tissues through water radiolysis, rather than metabolic oxidative imbalances, and initiate a DNA damage response activation of CDKN1A/P21, further elevating its levels and potentially exacerbating regenerative arrest. Although the mechanistic underpinnings of how ROS might activate *Cdkn1a* expression in space and during disuse remains elusive, various possibilities have been proposed, including that cold-inducible RNA binding protein CIRBP overexpression during spaceflight (Blaber et al., 2017) may function to stabilize *Cdkn1a* mRNAs through 3'UTR binding of the protein acting as a specific mRNA chaperonin (Roilo et al., 2018; Scoumanne et al., 2011). Single cell expression mapping in our study shows that *Cirbp* and *Cdkn1a* expression is co-downregulated in response to cyclic stretch in the early osteoblast wildtype cell cluster, supporting the hypothesis that CIRBP may act as *Cdkn1a* mRNAs chaperone regulated by mechanical loading and specifically induced by disuse. Studies of ground squirrel hibernation in which bone and muscle disuse is a factor also support this hypothesis, showing correlated elevation of *Cdkn1a* and *Cirbp* gene expression in bone marrow during torpor under elevated oxidative stress conditions (Cooper et al., 2016; Wei et al., 2018).

Decrease in physical activity is a common feature associated with the aging process, and spaceflight has been shown to have many tissue,

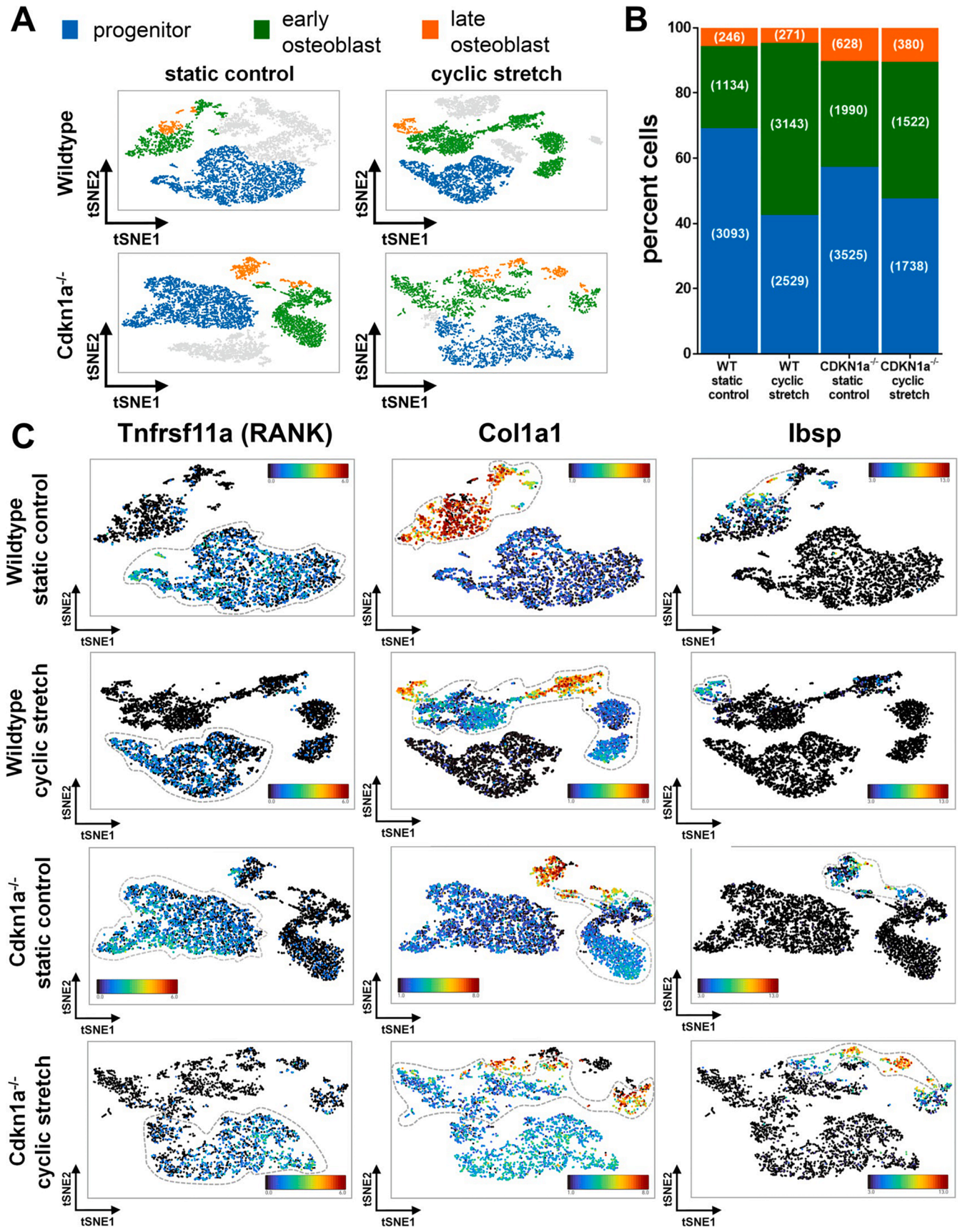

Figure 6. Single cell identification of osteoblast differentiation staging by biomarker clustering. Single cell t-SNE osteogenic staging clustering is shown in A). B) Cluster distribution and relative percentages of populations and cell numbers associated with each stage, showing that stretch stimulation induces transition of progenitor cells to early osteoblast commitment in both genotypes, but with *Cdkn1a*$^{-/-}$ clusters having greater numbers of late mineralizing osteoblasts. Panel C) shows representative markers (*Tnfrsf11a/Rank*, *Col1a1*, and *Ibsp*) of each differentiation stage for each genotype and loading condition.

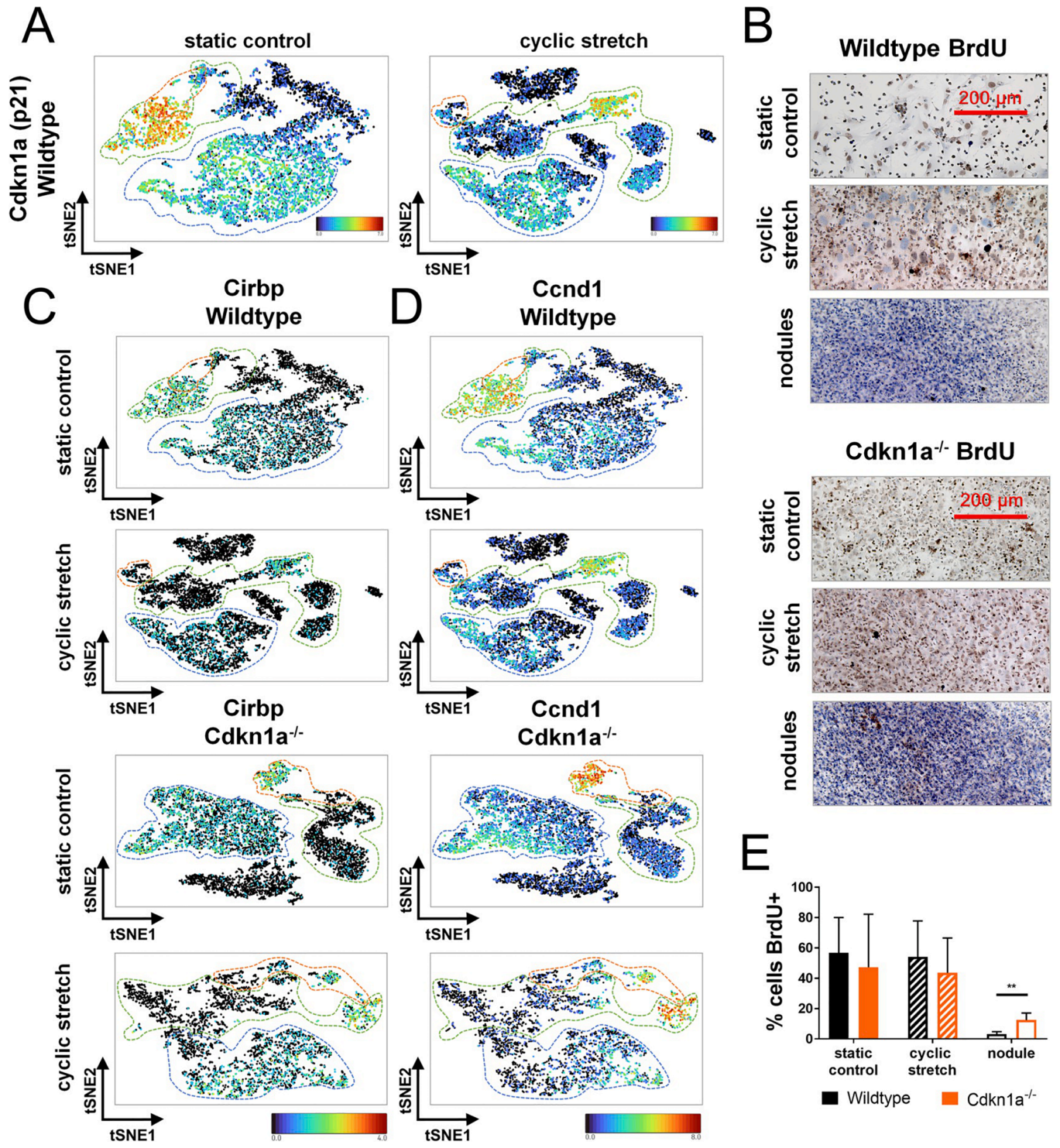

Figure 7. *Cdkn1a* expression is suppressed by cyclic stretch in wildtype osteoblasts, but not progenitors and *Cdkn1a* mechanical suppression or deletion results in increased proliferation. scRNA-seq mapping of *Cdkn1a*, *Cirbp* and cyclin D expression in the wildtype static control and cyclic stretch cultures is visualized in A) and C) and D). Maps show co-localization of mechanical suppression of *Cdkn1a* and *Cirbp* coupled with elevation of *Ccnd1*. *Ccnd1* expression in the *Cdkn1a*$^{-/-}$ cells show increased expression in early and late osteoblasts. B) shows greater cell number and BrdU incorporation with cyclic stretch in both cultures until cell density becomes three dimensional (nodules), at which point the *Cdkn1a*$^{-/-}$ cells stain positive for BrdU while minimal positive BrdU staining is identified in the wildtype cells. E) quantification of BrdU positive cells show at D9 of culture wildtype and *Cdkn1a*$^{-/-}$ cells are still highly proliferative. Only when the cells construct three dimensional nodules do the wildtype cells halt proliferation while the *Cdkn1a*$^{-/-}$ cells maintain proliferative ability.

cellular, and molecular disruptions comparable to accelerated aging. In addition, *Cdkn1a* expression, as well as other cell cycle checkpoint genes, show increased expression in aging tissues. Also, a recent study of *Cdkn1a* expression during dermis wound healing demonstrated that pharmacologic *Cdkn1a* silencing (siRNA) restored wound healing ability in aged mice to levels comparable to those in younger animals (Jiang et al., 2020). Further investigations have probed the wound healing abilities of the *Cdkn1a*-null mouse, finding that rather than wound healing based on scar tissue formation, the null mouse underwent scar-less regeneration and repair of the wound. Scar-less regeneration suggests that the deletion of *Cdkn1a* may release a proliferative restriction in differentiated tissue cells without loss of developmental-like re-patterning capacity, somewhat similar to the regenerative processes in amphibians (Arthur and Heber-Katz, 2011; Premnath et al., 2017). Our mineralizing culture experiments also exhibit a similar enhanced proliferative capacity in the *Cdkn1a*$^{-/-}$ primary marrow cells and show that upon induction of osteoblast differentiation production of mineral matrix comparable to the quality of their wildtype controls, but with a 7-day "jumpstart" in the development of mineralized tissue structure.

Regenerative tissue patterning is similar in many aspects to developmental patterning of embryogenesis, in which CDKN1A/P21-expressing cells, in proliferative arrest, act as secretory signaling centers and have been shown to mediate differential growth in the apical ectodermal ridge, hindbrain roof-plate, neural tube, pharyngeal arches, and gut endoderm (Guo et al., 2003; Li et al., 2018; Trokovic et al., 2005). Interestingly CDKN1A/P21-expressing cells in secretory signaling centers are arrested without induction of TRP53/P53, CDKN2A/P16 or CDKN2D/P19 DNA damage pathways, providing further evidence that CDKN1A/P21 may be a regulator of regenerative patterning and proliferative arrest independent of other DNA damage mediated cell cycle exit mechanisms. These CDKN1A/P21-expressing cells are protected from apoptosis transiently and release senescence associated secretory phenotype (SASP) factors which in turn elicit fate responses in surrounding cells (Vasey et al., 2011). In osteogenesis, SASP factors are principally produced by osteocytes, which function as regulatory controllers of bone resorption and formation, and in aging osteocytes *Cdkn1a* expression is elevated which correlates to reduced bone turnover and regenerative function (Farr et al., 2016). Additionally, an induced pluripotency study found that the cyclic forced expression of Yamanaka factors in aged animals reduced expression of TRP53/P53, CDKN1A/P21^{CIP1}, CDKN2A/P16^{INK4}, ATF3, IL6, and MMP13 and contributed to increased regeneration in muscle and pancreas tissues (Ocampo et al., 2016). Similar mechanisms including transient induction of proliferative arrest, expression of SASP and subsequent macrophage clearing is also present during limb regeneration in regenerative newts such as *Pleurodeles waltl*, but so far no clear *Cdkn1a* homologues have been identified in its genome (Elewa et al., 2017).

A critical mechanism in amphibian regeneration is the ability for cellular reprogramming, first reverting wound-adjacent cells to a "blastema" state of less specialization and increased proliferative capacity (de-differentiation) followed by subsequent re-differentiation into tissue specific cell types needed for functional tissue repatterning. Elimination of mammalian cell cycle arrest regulators, like CDKN1A/P21, significantly increases efficiency of induced pluripotency reprogramming (Banito et al., 2009; Hong et al., 2009) producing cells capable of extensive proliferation and functional commitment by mechanisms that may be similar to those in amphibian regeneration. Similarly, in our study, the finding that proliferating cells can be isolated from *Cdkn1a*$^{-/-}$ mineral nodules, also suggests that the absence of the gene may confer null tissues with increased regenerative ability compared to the *Cdkn1a*-expressing wildtype mineralized tissue. While we did not assess if the newly expanded culture could progress to complete osteogenic mineralization specialization, a previous spaceflight investigation using the embryoid body (EB) model suggested the state of *Cdkn1a* expression associated with spaceflight in microgravity primed EB cells for differentiation upon return to 1g (Blaber et al., 2015).

5. Conclusion

Collectively these studies provide evidence of CDKN1A/P21's role as a regulator of regenerative arrest and show that the deletion of this gene promotes differentiation progression, and elevates regenerative potential. Our results provide multiple lines of evidence that CDKN1A/P21 may act as a constitutive suppressor of osteogenic mechanotransduction, and that the *Cdkn1a*-null cultures show increased progenitor proliferation and osteoblast differentiation responsiveness to loading by cyclic stretch. Furthermore, re-plating of late mineralizing osteogenic cultures, BrdU proliferative marker assessment, plus single cell RNAseq results, show that deletion of *Cdkn1a* may release a stage specific transitional restriction between proliferative and differentiation states in bone marrow MSC-derived osteogenic progenitors undergoing *ex-vivo* mineralization. In total this work suggests a novel mechanistic framework for bone regenerative homeostasis in which CDKN1A/P21 plays a mechano-reversible anti-proliferative role during osteogenesis and could connect previous spaceflight results showing increased *Cdkn1a* expression in osteoprogenitors in microgravity, to the observed inhibition of regenerative bone formation in space (Morey and Baylink, 1978). More broadly this study also suggests that mechanical load suppression of *Cdkn1a* expression may contribute to the observed tissue regenerative benefits of load-bearing exercise.

Acknowledgements:

We thank NASA GeneLab Sequencing Group at NASA Ames Research Center (Moffett Field, CA), including V. Boyko and Dr. A. Seravia-Butler (NASA ARC) for technical assistance in scRNA-seq sample processing for sequencing and single cell sequence data QC and validation. We also thank Dr. Nancy Searby (NASA HQ), for the initial design and prototype iterations of the two-motor mechanical loading systems used in our studies (Searby, 2002). This work was supported by NASA Space Biology grants NNH14ZTT001N-0063 to Dr. E. Almeida, NNH14ZTT001N-0062 to Dr. E. Blaber, and a NASA Space Biology Postdoctoral Fellowship to Dr. C. Juran.

Author Contributions

C.M.J., E.A.B., and E.A.C.A. designed the experiments. C.M.J., E.A.B., M.C.-C., J.Z., and E.A.C.A. conducted the experiments, analyzed the data, and prepared the figures. C.M.J. and E.A.C.A. wrote the manuscript.

Appendix A. Supplementary data

Supplementary data to this article can be found online at https://doi.org/10.1016/j.scr.2021.102513.

References

Akima, H., Ushiyama, J.-I., Kubo, J., Fukuoka, H., Kanehisa, H., Fukunaga, T., 2007. Effect of unloading on muscle volume with and without resistance training. Acta Astronaut. 60 (8-9), 728–736.

Arthur, L., Heber-Katz, E., 2011. The role of p21 in regulating mammalian regeneration. Stem Cell Res. Ther. 2 (3), 30. https://doi.org/10.1186/scrt71.

Banito, A., Rashid, S.T., Acosta, J.C., Li, S., Pereira, C.F., Geti, I., Pinho, S., Silva, J.C., Azuara, V., Walsh, M., Vallier, L., Gil, J., 2009. Senescence impairs successful reprogramming to pluripotent stem cells. Genes Dev. 23 (18), 2134–2139.

Bedelbaeva, K., Snyder, A., Gourevitch, D., Clark, L., Zhang, X.-M., Leferovich, J., Cheverud, J.M., Lieberman, P., Heber-Katz, E., 2010. Lack of p21 expression links cell cycle control and appendage regeneration in mice. Proc. Natl. Acad. Sci. 107 (13), 5845–5850.

Bellosta, P., Masramon, L., Mansukhani, A., Basilico, C., 2003. p21WAF1/CIP1 acts as a brake in osteoblast differentiation. J. Bone Miner. Res. 18 (5), 818–826.

Berg, H.E., Eiken, O., Miklavcic, L., Mekjavic, I.B., 2007. Hip, thigh and calf muscle atrophy and bone loss after 5-week bedrest inactivity. Eur. J. Appl. Physiol. 99 (3), 283–289.

Blaber, E.A., Dvorochkin, N., Torres, M.L., Yousuf, R., Burns, B.P., Globus, R.K., Almeida, E.A.C., 2014. Mechanical unloading of bone in microgravity reduces

mesenchymal and hematopoietic stem cell-mediated tissue regeneration. Stem Cell Res. 13 (2), 181–201.
Blaber, E.A., Dvorochkin, N., Lee, C., Alwood, J.S., Yousuf, R., Pianetta, P., Globus, R.K., Burns, B.P., Almeida, E.A.C., Vanacker, J.-M., 2013. Microgravity induces pelvic bone loss through osteoclastic activity, osteocytic osteolysis, and osteoblastic cell cycle inhibition by CDKN1a/p21. PLoS ONE 8 (4), e61372.
Blaber, E.A., Finkelstein, H., Dvorochkin, N., Sato, K.Y., Yousuf, R., Burns, B.P., Globus, R.K., Almeida, E.A.C., 2015. Microgravity reduces the differentiation and regenerative potential of embryonic stem cells. Stem Cells Dev. 24 (22), 2605–2621.
Blaber, E., Pecaut, M., Jonscher, K., 2017. Spaceflight activates autophagy programs and the proteasome in mouse liver. Int. J. Mol. Sci. 18 (10), 2062. https://doi.org/10.3390/ijms18102062.
Boerckel, J.D., Kolambkar, Y.M., Stevens, H.Y., Lin, A.S.P., Dupont, K.M., Guldberg, R.E., 2012. Effects of in vivo mechanical loading on large bone defect regeneration. J. Orthop. Res. 30 (7), 1067–1075.
Cazzalini, O., Scovassi, A.I., Savio, M., Stivala, L.A., Prosperi, E., 2010. Multiple roles of the cell cycle inhibitor p21CDKN1A in the DNA damage response. Mutation Research/Reviews in Mutation Research 704 (1-3), 12–20.
Choudhury, A.R., Ju, Z., Djojosubroto, M.W., Schienke, A., Lechel, A., Schaetzlein, S., Jiang, H., Stepczynska, A., Wang, C., Buer, J., Lee, H.-W., von Zglinicki, T., Ganser, A., Schirmacher, P., Nakauchi, H., Rudolph, K.L., 2007. Cdkn1a deletion improves stem cell function and lifespan of mice with dysfunctional telomeres without accelerating cancer formation. Nat. Genet. 39 (1), 99–105.
Cooper, S.T., Sell, S.S., Fahrenkrog, M., Wilkinson, K., Howard, D.R., Bergen, H., Cruz, E., Cash, S.E., Andrews, M.T., Hampton, M., 2016. Effects of hibernation on bone marrow transcriptome in thirteen-lined ground squirrels. Physiol. Genomics 48 (7), 513–525.
D'Angelo, F., Tiribuzi, R., Armentano, I., Kenny, J.M., Martino, S., Orlacchio, A., 2011. Mechanotransduction: tuning stem cells fate. Journal of Functional Biomaterials 2 (2), 67–87.
Deng, C., Zhang, P., Wade Harper, J., Elledge, S.J., Leder, P., 1995. Mice lacking p21CIP1/WAF1 undergo normal development, but are defective in G1 checkpoint control. Cell 82 (4), 675–684.
Donehower, L.A., Harvey, M., Slagle, B.L., McArthur, M.J., Montgomery, C.A., Butel, J.S., Bradley, A., 1992. Mice deficient for p53 are developmentally normal but susceptible to spontaneous tumours. Nature 356 (6366), 215–221.
Dulić, V., Stein, G.H., Far, D.F., Reed, S.I., 1998. Nuclear accumulation of p21Cip1 at the onset of mitosis: a role at the G2/M-phase transition. Mol. Cell. Biol. 18 (1), 546–557.
Elewa, A., Wang, H., Talavera-López, C., Joven, A., Brito, G., Kumar, A., Hameed, L.S., Penrad-Mobayed, M., Yao, Z., Zamani, N., Abbas, Y., Abdullayev, I., Sandberg, R., Grabherr, M., Andersson, B., Simon, A., 2017. Reading and editing the Pleurodeles waltl genome reveals novel features of tetrapod regeneration. Nat. Commun. 8 (1) https://doi.org/10.1038/s41467-017-01964-9.
Fakhry, M., Hamade, E., Badran, B., Buchet, R., Magne, D., 2013. Molecular mechanisms of mesenchymal stem cell differentiation towards osteoblasts. World Journal of Stem Cells 5, 136.
Farr, J.N., Fraser, D.G., Wang, H., Jaehn, K., Ogrodnik, M.B., Weivoda, M.M., Drake, M. T., Tchkonia, T., LeBrasseur, N.K., Kirkland, J.L., Bonewald, L.F., Pignolo, R.J., Monroe, D.G., Khosla, S., 2016. Identification of senescent cells in the bone microenvironment. J. Bone Miner. Res. 31 (11), 1920–1929.
Gartel, A.L., Serfas, M.S., Gartel, M., Goufman, E., Wu, G.S., El-Deiry, W.S., Tyner, A.L., 1996. p21 (WAF1/CIP1) expression is induced in newly nondividing cells in diverse epithelia and during differentiation of the Caco-2 intestinal cell line. Exp. Cell Res. 227 (2), 171–181.
Guo, Q., Loomis, C., Joyner, A.L., 2003. Fate map of mouse ventral limb ectoderm and the apical ectodermal ridge. Dev. Biol. 264 (1), 166–178.
Guyot, Y., Smeets, B., Odenthal, T., Subramani, R., Luyten, F.P., Ramon, H., Papantoniou, I., Geris, L., McNamara, L.M., 2016. Immersed boundary models for quantifying flow-induced mechanical stimuli on stem cells seeded on 3D scaffolds in perfusion bioreactors. PLoS Comput. Biol. 12 (9), e1005108.
Haasper, C., Jagodzinski, M., Drescher, M., Meller, R., Wehmeier, M., Krettek, C., Hesse, E., 2008. Cyclic strain induces FosB and initiates osteogenic differentiation of mesenchymal cells. Exp. Toxicol. Pathol. 59 (6), 355–363.
Hong, H., Takahashi, K., Ichisaka, T., Aoi, T., Kanagawa, O., Nakagawa, M., Okita, K., Yamanaka, S., 2009. Suppression of induced pluripotent stem cell generation by the p53–p21 pathway. Nature 460 (7259), 1132–1135.
Jackson, R.J., Adnane, J., Coppola, D., Cantor, A., Sebti, S.M., Pledger, W.J., 2002. Loss of the cell cycle inhibitors p21 Cip1 and p27 Kip1 enhances tumorigenesis in knockout mouse models. Oncogene 21 (55), 8486–8497.
Jiang, D., Vries, J.C., Muschhammer, J., Schatz, S., Ye, H., Hein, T., Fidan, M., Romanov, V.S., Rinkevich, Y., Scharffetter-Kochanek, K., 2020. Local and transient inhibition of p21 expression ameliorates age-related delayed wound healing. Wound Repair and Regeneration 28 (1), 49–60.
Karimian, A., Ahmadi, Y., Yousefi, B., 2016. Multiple functions of p21 in cell cycle, apoptosis and transcriptional regulation after DNA damage. DNA Repair 42, 63–71.
Khayal, L.A., Grünhagen, J., Provazník, I., Mundlos, S., Kornak, U., Robinson, P.N., Ott, C.-E., 2018. Transcriptional profiling of murine osteoblast differentiation based on RNA-seq expression analyses. Bone 113, 29–40.
Lanyon, L.E., Goodship, A.E., Pye, C.J., MacFie, J.H., 1982. Mechanically adaptive bone remodelling. J. Biomech. 15 (3), 141–154.
Li, Y.i., Zhao, H., Huang, X., Tang, J., Zhang, S., Li, Y., Liu, X., He, L., Ju, Z., Lui, K.O., Zhou, B., 2018. Embryonic senescent cells re-enter cell cycle and contribute to tissues after birth. Cell Res. 28 (7), 775–778.
Martín-Caballero, J., Flores, J.M., García-Palencia, P., Serrano, M., 2001. Tumor susceptibility of p21Waf1/Cip1-deficient mice. Cancer Res. 61, 6234–6238.
Morey, E., Baylink, D., 1978. Inhibition of bone formation during space flight. Science 201 (4361), 1138–1141.
Ocampo, A., Reddy, P., Martinez-Redondo, P., Platero-Luengo, A., Hatanaka, F., Hishida, T., Li, M., Lam, D., Kurita, M., Beyret, E., 2016. In vivo amelioration of age-associated hallmarks by partial reprogramming. Cell 167 (1719–1733), e1712.
Parker, S., Eichele, G., Zhang, P., Rawls, A., Sands, A., Bradley, A., Olson, E., Harper, J., Elledge, S., 1995. p53-independent expression of p21Cip1 in muscle and other terminally differentiating cells. Science 267 (5200), 1024–1027.
Perhonen, M.A., Franco, F., Lane, L.D., Buckey, J.C., Blomqvist, C.G., Zerwekh, J.E., Peshock, R.M., Weatherall, P.T., Levine, B.D., 2001. Cardiac atrophy after bed rest and spaceflight. J. Appl. Physiol. 91 (2), 645–653.
Premnath, P., Jorgenson, B., Hess, R., Tailor, P., Louie, D., Taiani, J., Boyd, S., Krawetz, R., 2017. p21−/− mice exhibit enhanced bone regeneration after injury. BMC Musculoskeletal Disorders 18, 435.
Riley, D.A., Bain, J.L.W., Thompson, J.L., Fitts, R.H., Widrick, J.J., Trappe, S.W., Trappe, T.A., Costill, D.L., 2000. Decreased thin filament density and length in human atrophic soleus muscle fibers after spaceflight. J. Appl. Physiol. 88 (2), 567–572.
M. Roilo M.K. Kullmann L. Hengst Cold-inducible RNA-binding protein (CIRP) induces translation of the cell-cycle inhibitor p27Kip1 46 6 2018 2018 3198 3210.
Roukos, V., Pegoraro, G., Voss, T.C., Misteli, T., 2015. Cell cycle staging of individual cells by fluorescence microscopy. Nat. Protoc. 10 (2), 334–348.
A. Scoumanne S.J. Cho J. Zhang X. Chen The cyclin-dependent kinase inhibitor p21 is regulated by RNA-binding protein PCBP4 via mRNA stability 39 1 2011 2011 213 224.
Searby, N.D., 2002. Morphological responses of osteoblasts to mechanical loading: experimental and modeling studies. (Stanford University).
Stavenschi, E., Corrigan, M.A., Johnson, G.P., Riffault, M., Hoey, D.A., 2018. Physiological cyclic hydrostatic pressure induces osteogenic lineage commitment of human bone marrow stem cells: a systematic study. Stem Cell Res. Ther. 9, 1–13.
Swift, J., Ivanovska, I.L., Buxboim, A., Harada, T., Dingal, P.C.D.P., Pinter, J., Pajerowski, J.D., Spinler, K.R., Shin, J.-W., Tewari, M., Rehfeldt, F., Speicher, D.W., Discher, D.E., 2013. Nuclear lamin-A scales with tissue stiffness and enhances matrix-directed differentiation. Science 341 (6149), 1240104. https://doi.org/10.1126/science:1240104.
Takata, S., Yamashita, Y., Masaki, K., Morimoto, K., Nakano, M., 1993. Effects of bed rest on bone metabolism in patients with femoral neck fracture. The Annals of Physiological Anthropology 12 (6), 321–325.
Thomas, G.P., El Haj, A.J., 1996. Bone marrow stromal cells are load responsivein vitro. Calcif. Tissue Int. 58 (2), 101–108.
Titushkin, I., Cho, M., 2007. Modulation of cellular mechanics during osteogenic differentiation of human mesenchymal stem cells. Biophys. J . 93 (10), 3693–3702.
Trokovic, R., Jukkola, T., Saarimäki, J., Peltopuro, P., Naserke, T., Vogt Weisenhorn, D. M., Trokovic, N., Wurst, W., Partanen, J., 2005. Fgfr1-dependent boundary cells between developing mid-and hindbrain. Dev. Biol. 278 (2), 428–439.
Vasey, D.B., Roland Wolf, C., Brown, K., Whitelaw, C.B.A., 2011. Spatial p21 expression profile in the mid-term mouse embryo. Transgenic Res. 20 (1), 23–28.
Vining, K.H., Mooney, D.J., 2017. Mechanical forces direct stem cell behaviour in development and regeneration. Nat. Rev. Mol. Cell Biol. 18 (12), 728–742.
Wagers, A., 2012. The stem cell niche in regenerative medicine. Cell Stem Cell 10 (4), 362–369.
Wallace, I.J., Pagnotti, G.M., Rubin-Sigler, J., Naeher, M., Copes, L.E., Judex, S., Rubin, C.T., Demes, B., 2015. Focal enhancement of the skeleton to exercise correlates with responsivity of bone marrow mesenchymal stem cells rather than peak external forces. J. Exp. Biol. 218, 3002–3009.
Wei, Y., Zhang, J., Xu, S., Peng, X., Yan, X., Li, X., Wang, H., Chang, H., Gao, Y., 2018. Controllable oxidative stress and tissue specificity in major tissues during the torpor–arousal cycle in hibernating Daurian ground squirrels. Royal Society Open Biology 8 (10), 180068. https://doi.org/10.1098/rsob.180068.
Weinberg, W.C., Fernandez-Salas, E., Morgan, D.L., Shalizi, A., Mirosh, E., Stanulis, E., Deng, C., Hennings, H., Yuspa, S.H., 1999. Genetic deletion of p21WAF1 enhances papilloma formation but not malignant conversion in experimental mouse skin carcinogenesis. Cancer Res. 59, 2050–2054.
Yosef, R., Pilpel, N., Papismadov, N., Gal, H., Ovadya, Y., Vadai, E., Miller, S., Porat, Z., Ben-Dor, S., Krizhanovsky, V., 2017. p21 maintains senescent cell viability under persistent DNA damage response by restraining JNK and caspase signaling. EMBO J 36, 2280–2295.